

Noname manuscript No.
(will be inserted by the editor)

A multi-objective constrained POMDP model for breast cancer screening

Can Kavaklıoglu · Mucahit Cevik · Robert
Helmeczi · Davood Pirayesh Neghab

Received: date / Accepted: date

Abstract Breast cancer is a common and deadly disease, but it is often curable when diagnosed early. While most countries have large-scale screening programs, there is no consensus on a single globally accepted policy for breast cancer screening. The complex nature of the disease; limited availability of screening methods such as mammography, magnetic resonance imaging (MRI), and ultrasound screening; and public health policies all factor into the development of screening policies. Resource availability concerns necessitate the design of policies which conform to a budget, a problem which can be modelled as a constrained partially observable Markov decision process (CPOMDP). In this study, we propose a multi-objective CPOMDP model for breast cancer screening with two objectives: minimize the lifetime risk of dying due to breast cancer and maximize the quality-adjusted life years. Additionally, we consider an expanded action space which allows for screening methods beyond mammography. Each action has a unique impact on quality-adjusted life years and lifetime risk, as well as a unique cost. Our results reveal the Pareto frontier of optimal solutions for average and high risk patients at different budget levels, which can be used by decision makers to set policies in practice.

Keywords Markov decision processes, Constrained POMDPs, Breast cancer screening, Medical decision making

Can Kavaklıoglu
Ryerson University, Toronto, Canada

Mucahit Cevik
Ryerson University, Toronto, Canada
E-mail: mcevik@ryerson.ca

Robert Helmeczi
Ryerson University, Toronto, Canada

Davood Pirayesh Neghab
Ryerson University, Toronto, Canada

1 Introduction

Breast cancer is the most commonly occurring cancer among women and is the second leading cause of cancer death (DeSantis et al., 2019). Siegel et al. (2020) estimated that among US women, there would be 285,360 new deaths by cancer in 2020, 14.9 % of which would be from breast cancer. While the incidence of breast cancer has increased by 30% (62% of which were localized breast cancers) from 1975 to 2010, its associated mortality rate has declined by 34% (Narod et al., 2015). This decline can be attributed to improvements in treatment such as surgery and radiation for non-metastatic breast cancers (Waks and Winer, 2019). However, the pace of this decline has slowed from an annual decrease of 1.9% during 1998 through 2011 to 1.3% during 2011 through 2017 (DeSantis et al., 2019). A possible reason for this is that, despite advancements in non-metastatic breast cancer treatments, treatments for metastatic cancers are rarely permanent (Waks and Winer, 2019). Furthermore, when a patient self-diagnoses breast cancer, the cancer is typically already metastasized. Thus, early diagnosis could be crucial to accelerate the decline in mortality rates for this disease.

Various screening methods are used to diagnose breast cancer, with the most common approach being mammography. Mammography is capable of detecting breast cancer years before physical symptoms develop, and so its usage contributes to lower mortality rates. The five-year breast cancer survival rate in countries with population-based screening programs (e.g., North America, Sweden, and Japan) is over 80%, while it is less than 40% in low-income countries that do not have established screening programs (Coleman et al., 2008). Moreover, breast cancers detected with mammography (as compared to physical examination) are generally non-metastatic and more likely to be treated with breast surgery (56% compared to 32%), and less likely to receive adjunct chemotherapy (28% compared to 56%), resulting in lower overall costs of treatment (Barth Jr et al., 2005).

Despite its effectiveness in early diagnosis and lowering mortality rates, mammography is not without its downsides. Firstly, mammography screenings are expensive: it was estimated that the total cost of mammography screenings in the United States in 2010 was \$7.8 billion (O'Donoghue et al., 2014). Secondly, a significant percentage of mammography screenings result in false positives. Fuller et al. (2015) conducted a simulation study which showed that out of 10,000 women undergoing annual mammography screenings, 4,970 to 6,130 of them receive at least one false positive result over 10 years, with 700 to 980 resulting in an unnecessary biopsy. Another study estimates that the cumulative risk of a false positive after 10 mammograms is 49.1%, as compared to 22.3% after 10 clinical breast exams (Elmore et al., 1998). False positives result in unnecessary anxiety for patients and additional costs for follow-up procedures.

While there have been advancements in mammography technology, about 20% of mammography screenings still result in false negatives, which are much more common among women with dense breasts (ACS, 2019). Mammographies are also less successful at detecting breast cancer in women with BRCA1 and BRCA2 mutations (Tilanus-Linthorst et al., 2002). Supplemental tests with a higher sensitivity compared to mammography, such as MRI, can be used to screen women with a higher risk of developing breast cancer. For instance, ACS (2019) recommends women with a lifetime breast cancer risk of 20% or more undergo supplemental MRI screening in the case of negative mammography results. However, these

supplemental tests incur an additional cost and increase the likelihood of false positives, making them a potentially undesirable alternative.

In summary, the risk of false positives and false negatives, as well as the prohibitive cost of screenings, complicate the task of designing a policy for the breast cancer screening problem. Additionally, the risk of developing breast cancer is not equal among women, as the sensitivity of screenings is heavily dependent on both genetics and breast density. To address these issues, we formulate a multi-objective CPOMDP model resulting in a personalized, budget-constrained screening policy that maximizes a patient's QALYs while minimizing her lifetime risk of dying due to breast cancer.

Our paper's contribution can be viewed from both methodological and practical standpoints. In terms of methodology, we extend the CPOMDP framework proposed by Cevik et al. (2018) by incorporating multiple objectives to assess the trade-off between QALYs and lifetime breast cancer risk. In addition, we empirically show that CPOMDP algorithm run times can be improved substantially by identifying the relevant belief states at each decision epoch. From a practical point of view, we propose a more comprehensive modelling framework to increase early detection rates and QALYs while reducing lifetime risk. We accomplish this by considering supplemental tests in addition to mammography. Our numerical study shows that supplemental tests are frequently recommended for higher risk patient groups. In addition, we show the Pareto frontier over the QALY maximization and lifetime risk minimization objectives, which help understanding the trade-offs between these two important modelling objectives.

The rest of the paper is organized as follows. Section 2 provides a brief discussion of the literature surrounding cancer screening and similar modelling frameworks. Section 3 provides the mathematical background for the CPOMDP methodology, which is followed up by our proposed model. The results are then presented in Section 4, followed by Section 5 where we discuss our findings and future research directions.

2 Literature Review

Different methodologies have been employed to solve cancer screening problems including simulation-based (Mandelblatt et al., 2016; Sprague et al., 2015) and optimization-based techniques (Saville et al., 2019). Several studies have been conducted to determine efficient cancer-screening policies by evaluating their cost-effectiveness using Markov models (Le, 2016; Ralaidovy et al., 2018; Gopalappa et al., 2018; Bansal et al., 2020). Tollens et al. (2021) assessed the rate of false positive outcomes in two rounds of screening of women with extremely dense breasts and evaluated their impact on cost-effectiveness. Kaiser et al. (2021a,b) employed Markov models to evaluate cumulative costs, QALY, false positive, and false negative results of breast cancer screening and conducted deterministic and probabilistic analyses to test the model stability.

Some other studies developed simulation-based analysis using partially observable Markov chain (POMC) models. For example, Maillart et al. (2008) and Madadi et al. (2015) assessed breast cancer screening policies where the former focuses on balancing cost-effectiveness with lifetime mortality risk, and the latter focuses on the impact of patient adherence to screening recommendations.

Similarly, Molani et al. (2019) developed POMC models to examine the risks of various screening policies while considering a patient's adherence behavior. Later, Molani et al. (2020) formulated a POMC model to study the effectiveness of supplemental screening (e.g., ultrasound) while incorporating the impact of radiologists' bias on patients' screening outcomes. POMC models have also been used for other cancer types. For instance, Li et al. (2014) developed POMC models to evaluate colorectal cancer screening policies among others. While these studies comprehensively evaluate the impacts of various factors such as screening age and intervals, they do not attempt to find optimal policies.

A strand of the literature develops optimization-based techniques to find policies for various cancer screening problems. For instance, Akhavan-Tabatabaei et al. (2017) optimized cervical cancer screening decisions by modelling the problem as a Markov decision process (MDP), accounting for several factors such as a patient's age and screening results. Similarly, Chhatwal et al. (2010) and Alagoz et al. (2013) optimized the post-mammography biopsy decisions for breast cancer using MDPs. Vargas et al. (2015) incorporated the impact of over-treatment and the potential delay in cancer detection into an MDP model of the breast cancer screening problem. Ayvaci et al. (2018) developed a stochastic modelling framework using MDPs to optimize risk-sensitive diagnostic decisions after a mammography exam by considering the variations in risk preferences of the individuals. Tunc et al. (2018) optimized breast cancer diagnostic decisions to reduce the overdiagnosis costs in a patient's lifetime based on cancer subtypes using a large-scale MDP model with many finite states. Imani et al. (2020) designed an MDP model to optimize the costs and the QALYs for breast cancer treatment plans considering prophylactic surgery, radiation therapy, chemotherapy, and their combinations. On the other hand, in most cases, a patient's state is not fully observable, and therefore partially observable MDPs (POMDPs), while more difficult to solve due to a generally intractable state space, are more suitable for modelling the cancer screening problem since they capture the uncertainty related to the imperfect state information. POMDPs have been used to develop policies for a wide variety of cancer screening problems such as prostate (Zhang et al., 2012a,b; Zhang and Denton, 2018; Li et al., 2021), colorectal (Erenay et al., 2014), liver (Chen et al., 2018), cervical (Ebadi and Akhavan-Tabatabaei, 2021), and lung cancers (Petousis, 2019).

Numerous studies have specifically investigated the breast cancer screening problem. Ayer et al. (2012) proposed a finite-horizon POMDP to identify policies for patients based on their risk factors. Ayer (2015) and Ayer et al. (2016) formulated the breast cancer screening problem using POMDPs, where the former focuses on finding the optimal screening policy for given sensitivity and specificity values, and the latter incorporates both the patient's adherence behavior and their breast cancer risk into the decision process. Otten et al. (2017) and Witteveen et al. (2018) proposed a POMDP model for breast cancer and considered the personal risk of developing cancer to investigate the resource allocation for optimal and personal follow-up. Additionally, Sandikci et al. (2018) evaluated the impact of supplemental screenings by sequentially considering the screening decisions. That is, their model first determines whether the patient should receive mammography, and the supplemental screening decision is then made according to the mammography outcome. In a recent study, Hajjar and Alagoz (2022) developed a model to identify the optimal screening decisions for an index disease (e.g., breast cancer) while incorporating a chronic condition (e.g. diabetes). In par-

ticular, they provided personalized breast cancer screening recommendations for women with diabetes and found several remarkable policy insights for this case. Other extensions to this context include formulating a POMDP with continuous states. For example, Otten et al. (2020) extended the study by Otten et al. (2017) to a continuous state problem by modelling the size of the tumor as a continuous valued component in the state space, which is based on the assumption that tumor growth follows an exponential distribution. Horiguchi (2021) also evaluated the periodic screening programs for breast cancer by converting a POMDP to a fully observable MDP with a continuous state space.

The optimization approaches discussed so far assume that the decision maker has infinite resources, which is generally not the case. Hence, it is often useful to find optimal policies that satisfy certain constraints, such as limited screening resources. Several studies have proposed using constrained MDP models for different cancer screening problems (Ayvacı et al., 2012; Lee et al., 2019). Poupart et al. (2015) and Lee et al. (2018) devised solution methods for constrained POMDPs (CPOMDPs) based on approximate linear programming and Monte Carlo tree search, respectively. Many CPOMDP applications followed, especially in the healthcare domain. Gan et al. (2019) investigated opioid use disorder using CPOMDP models, and imposed restrictions on the available budget for interventions and surveillance (e.g., using wearable devices). To account for the imperfect patient state information and budgetary constraints in the breast cancer screening problem, Cevik et al. (2018) proposed a finite-horizon CPOMDP model that maximizes patient QALYs while limiting the number of mammographies received during the patient’s lifetime. In this study, we extend Cevik et al. (2018)’s work by introducing supplemental screening tests to the decision process and investigating multi-objective optimization approaches for the breast cancer screening problem. Different from Sandikci et al. (2018), we consider only the simultaneous usage of supplemental tests with mammography, which help simplifying the problem for the CPOMDP framework. Table 1 summarizes the relevant studies in the literature and demonstrate the relative positioning of our work.

3 Methodology

In this section, we first present the preliminaries and the POMDP model for the breast cancer screening problem. We then propose a multi-objective CPOMDP model that simultaneously optimizes a patient’s QALYs and lifetime mortality risk, subject to a budget constraint. Finally, we formulate a linear programming model to approximate the multi-objective CPOMDP model.

3.1 Preliminaries

A discrete-time finite horizon POMDP model is defined as a seven tuple $\langle \mathcal{T}, \mathcal{S}, \mathcal{A}, \mathcal{O}, \mathcal{R}, \mathcal{P}, \mathcal{Z} \rangle$. Each model component describes one aspect of the environment in which a decision maker — referred to as *the agent* — takes actions and makes observations. We use \mathcal{T} to denote the set of decision epochs and \mathcal{S} to denote the set of core states, which represents the partially observable states that the agent can occupy. At each decision epoch, the agent takes an action $a \in \mathcal{A}$

Table 1: Summary of the most relevant studies in the literature.

Research	Problem/ Cancer Type	Objective	Model Specification		Solution Approach
			Constraint	Framework	
Chhatwal et al. (2010)	Breast	QALY	None	MDP	DP
Zhang et al. (2012a)	Prostate	QALY	None	PMDP	DP
Ayvaci et al. (2012)	Breast	QALY	Budget	MDP	MIP
Ayer et al. (2012)	Breast	QALY	None	POMDP	DP
Alagoz et al. (2013)	Breast	QALY	None	MDP	DCL
Erenay et al. (2014)	Colorectal	QALY	None	POMDP	LP
Ayer et al. (2016)	Breast	QALY	None	POMDP	LP
Akhavan-Tabatabaei et al. (2017)	Cervical	Cost	None	MDP	DP
Chen et al. (2018)	Liver	Cost effectiveness	None	MDP	MIP
Cevik et al. (2018)	Breast	QALY	No. of screenings	POMDP	MILP
Çağlayan et al. (2018)	Breast	QALY	Budget	POMDP	MILP
Lee et al. (2019)	Liver	Early-stage detections	Screening resources	POMDP	BIP
Gan et al. (2019)	OUD	QALD	Budget	POMDP	DP
Our Study	Breast	QALY and Risk	Budget	POMDP	MILP

OUD: Opioid Use Disorder, DP: Dynamic Programming, MIP: Mixed-Integer Programming, DCL: Double-Control Policy, LP: Linear Programming, MILP: Mixed-Integer Linear Programming, BIP: Binary Integer Programming

and makes an observation $\theta \in \mathcal{O}$. Observations and transitions to new states are uncertain, and are therefore described by probabilities. That is, $p_{ij}^{ta} \in \mathcal{Z}$ represents the probability that the agent will transition from state $i \in \mathcal{S}$ to $j \in \mathcal{S}$ when action $a \in \mathcal{A}$ is taken at time $t \in \mathcal{T}$, and $z_{i\theta}^{ta} \in \mathcal{Z}$ represents the probability that the agent will observe $\theta \in \mathcal{O}$ after taking action $a \in \mathcal{A}$ in state $i \in \mathcal{S}$ at time $t \in \mathcal{T}$. The agent collects rewards throughout the decision process according to $\omega_i^{ta} \in \mathcal{R}$, which denotes the reward for performing action $a \in \mathcal{A}$ in state $i \in \mathcal{S}$ at time $t \in \mathcal{T}$. Table 2 summarizes the notation used in our study.

As the state space is only partially observable, the POMDP agent cannot know its core state with certainty. Instead, the agent maintains a *belief state*: a probability distribution over the set of core states \mathcal{S} . The belief state $\boldsymbol{\pi} \in \Pi(\mathcal{S})$ is an $|\mathcal{S}|$ -dimensional vector where π_i gives the probability that the agent is in the state $i \in \mathcal{S}$, that is,

$$\Pi(\mathcal{S}) = \{\boldsymbol{\pi} \mid \sum_{i \in \mathcal{S}} \pi_i = 1, \pi_i \geq 0, \forall i \in \mathcal{S}\}.$$

At each decision epoch $t \in \mathcal{T}$, as the agent takes an action $a \in \mathcal{A}$, and makes an observation $\theta \in \mathcal{O}$, its belief state is updated from $\boldsymbol{\pi}$ to $\boldsymbol{\pi}'$ according to Bayes'

Table 2: Notation used for the parameters and the mathematical formulas.

Notation	Description
$t \in \mathcal{T}$	a decision epoch from the set of decision epochs
$i \in \mathcal{S}$	a state in the state space
$a \in \mathcal{A}$	an action in the action space
$\theta \in \mathcal{O}$	an observation in the observation space
$\pi \in \Pi(\mathcal{S})$	a belief state in the belief space
$W, M, M\&R, M\&U$	wait, mammography, mammography + MRI, mammography + ultrasound actions
$p_{ij}^{ta} \in \mathcal{P}$	probability of making a transition from state i to state j by taking action a at time t , and the corresponding probability space
$z_{j\theta}^{ta} \in \mathcal{Z}$	probability of making a observation θ at state j by taking action a at time t , and the corresponding probability space
$\omega_i^{ta} \in \mathcal{R}$	immediate rewards for QALYs for taking action a at state i and time t , and the corresponding reward space
ϕ_i^t, φ_i	salvage reward at time t , and terminal reward for state $i \in \mathcal{S}$
$\Delta^{Scr}, \Delta^{TP}, \Delta^{FP}$	disutilities for screening, TP, and FP test results
$Q_t^a(\pi), \hat{Q}_t^a(\pi)$	optimal and approximate value functions for belief state π at time t
$\mu \in \Upsilon$	a policy and set of policies
γ_i^{ta}	immediate reward for breast cancer risk corresponding to state i , action a and time t
c_i^{ta}	cost of taking action a at state i and time t
C	budget limit
$b \in \mathcal{G}$	a grid point and set of grid points
\mathcal{K}	index set for the grid points
$\beta_{k\ell}^{ta\theta}$	convex combination weight for the grid point b^ℓ for the updated belief state $(b^k)'$ when the update is performed based on action a and observation θ at time t
$\rho, \boldsymbol{\rho} = [\rho_1, \dots, \rho_n]$	resolution value and resolution vector used for grid construction
$\psi = [\psi_1, \dots, \psi_n]$	resolution threshold vector used to partition the belief space
$f_{k\ell}^{ta}$	probability of transitioning from belief state b^ℓ to the belief state b^k by taking action a at t
x_{tka}	state-action occupancy measures, i.e., the probability of occupying belief state $b^k \in \mathcal{G}$ and taking action a at time t
h_1, h_2	expected total QALYs and expected total life-time risk
δ_k	probability of occupying grid point b^k at the first decision epoch
ν_{tka}	binary variable with value one if action a is taken at belief state $b^k \in \mathcal{G}$ at time t
q_{ti}	probability of death by cancer post-diagnosis for a patient diagnosed at state i at time t

rule, where

$$\pi'_j = \frac{\sum_i \pi_i z_{i\theta}^{ta} p_{ij}^{ta}}{\sum_{i,j} \pi_i p_{ij}^{ta} z_{i\theta}^{ta}} \quad (1)$$

gives the updated probability that the agent is in state $j \in \mathcal{S}$. The Bellman optimality equation (i.e., value function) corresponding to action $a \in \mathcal{A}$ can be obtained as

$$Q_t^a(\pi) = \sum_{i \in \mathcal{S}} \pi_i (\omega_i^{ta} + \lambda \sum_{\theta \in \mathcal{O}} \sum_{j \in \mathcal{S}} z_{j\theta}^{ta} p_{ij}^{ta} Q_{t+1}^*(\pi')), \quad (2)$$

where $Q_t^*(\pi) = \max_{a \in \mathcal{A}} \{Q_t^a(\pi)\}$ and λ is the discount factor. In finite horizon problems, λ is typically set to one.

3.2 CPOMDP Model for Breast Cancer Screening

We formulate a CPOMDP model for the breast cancer screening problem to optimize the screening decisions made by a decision maker (e.g., a radiologist or a physician) at each age between the ages of 40 to 100 (i.e., $\mathcal{T} = \{1, 2, \dots, 60\}$). Below, we first describe the CPOMDP model components, then formally define the multi-objective CPOMDP model.

- **Core states:** We choose the core states of the model to represent an individual’s health status. We consider a patient to be occupying one of the following states: healthy, having early-stage (i.e., in-situ) cancer, having late-stage (i.e., invasive) cancer, death due to breast cancer, and death from other causes. Our model considers the last two states as the fully observable terminal states, where the patient leaves the decision process. For simplicity, we map each core state to an integer, and represent the complete core state space as $\bar{\mathcal{S}} = \{0, 1, 2, 3, 4\}$, corresponding to the five states given above. Similarly, the partially observable state space is defined as $\mathcal{S} = \{0, 1, 2\}$. Consequently, the belief state π defined over the partially observable states is an $|\mathcal{S}|$ -tuple, storing the probability of a patient being healthy, having in-situ cancer, or having invasive cancer.
- **Actions and observations:** We consider three screening actions in our model, namely, mammography (\mathbb{M}), mammography supplemented with MRI ($\mathbb{M}\&\mathbb{R}$), and mammography supplemented with ultrasound ($\mathbb{M}\&\mathbb{U}$). We also include a wait action (\mathbb{W}) to indicate no screening is received at a given decision epoch. Accordingly, the action space is $\mathcal{A} = \{\mathbb{W}, \mathbb{M}, \mathbb{M}\&\mathbb{R}, \mathbb{M}\&\mathbb{U}\}$. When an action is taken, the associated observation is either positive (indicating that the patient has cancer) or negative (indicating that the patient is cancer-free), which leads to the observation space of $\mathcal{O} = \{\theta^-, \theta^+\}$. For the wait action, a positive observation can be attributed to self-detection or a clinical breast exam (e.g., feeling a lump in the breast tissue), whereas the observations for screening actions are the direct outcomes of the screening tests. The received observation can be a true positive (TP), true negative (TN), false positive (FP), or false negative (FN) result, depending on the underlying state of the patient.
- **Transition and observation probabilities:** Transition probabilities capture the transitions between the core states. As indicated by Maillart et al. (2008)’s study, the transition probabilities for the breast cancer screening problem possess several distinguishing properties. Firstly, the transition probabilities are time-dependent, as the probability of developing breast cancer increases with age (Maillart et al., 2008). Secondly, the transition probability matrices are upper diagonal, as a patient cannot recover from cancer during the decision process, i.e., once the patient is diagnosed with cancer, she leaves the decision process and does not return either. Lastly, the transition probabilities are action-independent, that is, $p_{ij}^{ta} = p_{ij}^t$, $\forall a \in \mathcal{A}$. Observation probabilities are linked to the performance (i.e., specificity and sensitivity) of the underlying action (e.g., screening test). Let $spec^{ta}$ and $sens^{ta}$ be the specificity and sensitivity parameters for action $a \in \mathcal{A}$ at time $t \in \mathcal{T}$, respectively. Accordingly, $z_{0\theta^-}^{ta} = spec^{ta}$, $z_{0\theta^+}^{ta} = (1 - spec^{ta})$, $z_{i\neq0,\theta^-}^{ta} = (1 - sens^{ta})$, and $z_{i\neq0,\theta^+}^{ta} = sens^{ta}$.
- **Rewards and costs:** In the breast cancer screening problem, the rewards are typically expressed in terms of QALY values. Immediate re-

wards, ω_i^{ta} , correspond to the QALY values associated with action a for a patient in state i at time t . These are calculated by taking into account the probability of death in a given decision epoch, as well as various disutilities associated with the actions. Assuming that there are no disutilities associated with the wait action, its corresponding expected immediate reward can be calculated using a half-cycle correction method, that is, $\omega_i^{t\mathbb{W}} = 1 \times \text{Pr}(\text{patient is alive at } t+1|\text{patient is alive at } t) + 0.5 \times \text{Pr}(\text{patient is dead at } t+1|\text{patient is alive at } t)$ (Gray et al., 2011). Immediate rewards for other actions can be derived from $\omega_i^{t\mathbb{W}}$. Let Δ^{Scr} , Δ^{TP} , and Δ^{FP} correspond to the screening, TP test, and FP test disutilities, respectively. We obtain the immediate rewards for the negative test results as $\omega_{i\theta^-}^{ta} = \omega_i^{t\mathbb{W}} - \Delta^{Scr}$ for $a \in \mathcal{A} \setminus \mathbb{W}$. Similarly, we obtain the immediate rewards for the positive test results, $\omega_{i\theta^+}$, by adjusting for the TP (i.e., when $i \neq 0, \theta = \theta^+$) and FP (i.e., when $i = 0, \theta = \theta^+$) test disutilities.

For screening, disutility values are typically low (e.g., 0.5 days for undergoing screening), whereas positive test results lead to additional procedures such as biopsies, incurring much higher disutility values (e.g., 2–4 weeks) (Ayer et al., 2012). Terminal rewards, φ_i , $i \in \mathcal{S}$, are received when a patient reaches time step T , whereas salvage rewards, ϕ_i , $i \neq 0$, are received when a patient is diagnosed with cancer to account for the utility of a possible recovery.

We consider the lifetime breast cancer risk (denoted by γ_i^{ta}) as another reward component, which corresponds to the risk of dying because of breast cancer if the patient is in state i at time t and takes action a . Lastly, we consider screening actions to have associated monetary costs, \mathbb{M} being the cheapest and $\mathbb{M\&R}$ being the most expensive option. Cost values, c^a for $a \in \mathcal{A}$, are independent of the state and time step.

In finite horizon CPOMDPs, the objective is to maximize the total expected reward, subject to a budget constraint. In our problem, we consider two separate objectives: maximization of the QALYs, and minimization of the lifetime breast cancer mortality risk. For a given starting belief state π^0 , this can be characterized as follows:

$$\max_{\mu \in \Upsilon} \left\{ E_{\pi^0}^{\mu} \left[\sum_{t=0}^{T-1} \omega_t(X_t, Y_t) + \omega_T(X_T) \right], E_{\pi^0}^{\mu} \left[- \sum_{t=0}^{T-1} \gamma_t(X_t, Y_t) - \gamma_T(X_T) \right] \right\}, \quad (3a)$$

$$\text{s.t. } E_{\pi^0}^{\mu} \left[\sum_{t=0}^{T-1} c_t(X_t, Y_t) \right] \leq C, \quad (3b)$$

where X_t and Y_t denote the states and actions at time t , respectively; Υ represents the set of all policies; and $\mu \in \Upsilon$ is a policy from the policy space. Similar to (2), the two optimization objectives in (3a) can be represented using Bellman optimality equations for unconstrained POMDP problems, and are typically solved using iterative optimization routines such as value iteration and backward induction methods (Puterman, 2014; Cevik et al., 2018). However, constrained MDP and POMDP models are usually formulated as (approximate) linear programs, the latter involving a grid-based approximation mechanism. Accordingly, we next review the grid-based approximations for POMDPs and then formulate our linear programming model to approximate the CPOMDP model presented in (3).

3.3 Grid-based Approximation Mechanism for CPOMDPs

A commonly used approach to approximate $Q_t^*(\boldsymbol{\pi})$ is to discretize $\Pi(\mathcal{S})$ into a set of grid points and calculate the values for only these grid points. We denote this set of grid points as $\mathcal{G} = \{\mathbf{b}^k \mid k \in \mathcal{K}\}$, where $\mathcal{K} = \{1, \dots, |\mathcal{G}|\}$ is index set of \mathcal{G} . Specifically, an approximate POMDP value function can be obtained for $b \in \mathcal{G}$ and $a \in \mathcal{A}$ as (Lovejoy, 1991):

$$\hat{Q}_t^a(\mathbf{b}) = \sum_{i \in \mathcal{S}} b_i \omega_i^{ta} + \sum_{i \in \mathcal{S}} b_i \sum_{\theta \in \mathcal{O}} \sum_{j \in \mathcal{S}} z_{i\theta}^{ta} p_{ij}^{ta} \sum_{k \in \mathcal{K}} \beta_k \hat{Q}_{t+1}(\mathbf{b}^k), \quad (4)$$

where $Q_{t+1}^*(\mathbf{b}') \approx \sum_{k \in \mathcal{K}} \beta_k \hat{Q}_{t+1}(\mathbf{b}^k)$. In this approximation, $\mathbf{b}' \notin \mathcal{G}$ is represented as a convex combination of the elements in \mathcal{G} , in which β_k gives the coefficient of \mathbf{b}^k , $k \in \mathcal{K}$. There are several different strategies for calculating these β -values; in this paper, we employ the LP-based approach provided by Sandikçi (2010).

3.3.1 Grid construction

The grid set \mathcal{G} can have a significant impact on the approximation quality, as was shown by Sandikçi et al. (2018) in the case of an unconstrained POMDP model for a similar breast cancer screening problem. In uniform grid construction methods, a resolution value, ρ , is used to construct the grid set. When a fixed resolution value is employed for this method, the number of grid points can be obtained as $\binom{|\mathcal{S}|-1+\rho}{\rho}$. For instance, for a problem with $|\mathcal{S}| = 3$, a fixed resolution value of $\rho = 2$ leads to $\mathcal{G}^{\text{fixed}} = \{[1, 0, 0], [1/2, 1/2, 0], [1/2, 0, 1/2], [0, 1, 0], [0, 1/2, 1/2], [0, 0, 1]\}$. However, in the breast cancer screening problem, it is important to pay closer attention to the parts of the belief space where the patient is more likely to be healthy. This is mainly because the probability of getting cancer on a specific time step is typically low, as indicated by the transition probability values. Accordingly, we follow the suggestions of Cevik et al. (2018) and Sandikçi et al. (2018), and employ a variable resolution uniform grid construction method for generating the grid points. In this approach, the resolution value varies based on a set of thresholds over the belief state components. For instance, for $|\mathcal{S}| = 3$, using a resolution value of $\rho = 4$ when $\pi_0 \in [1, 0.5]$ and a different resolution value of $\rho = 2$ when $\pi_0 \in (0.5, 1]$ leads to the grid set

$$\mathcal{G}^{\text{variable}} = \left\{ \begin{bmatrix} 1 \\ 0 \\ 0 \end{bmatrix}, \begin{bmatrix} \frac{3}{4} \\ \frac{1}{4} \\ 0 \end{bmatrix}, \begin{bmatrix} \frac{3}{4} \\ 0 \\ \frac{1}{4} \end{bmatrix}, \begin{bmatrix} \frac{1}{2} \\ \frac{1}{2} \\ 0 \end{bmatrix}, \begin{bmatrix} \frac{1}{2} \\ \frac{1}{4} \\ \frac{1}{4} \end{bmatrix}, \begin{bmatrix} \frac{1}{2} \\ 0 \\ \frac{1}{2} \end{bmatrix}, \begin{bmatrix} 0 \\ 1 \\ 0 \end{bmatrix}, \begin{bmatrix} 0 \\ \frac{1}{2} \\ \frac{1}{2} \end{bmatrix}, \begin{bmatrix} 0 \\ 0 \\ 1 \end{bmatrix} \right\}.$$

That is, we end up with 9 grid points using this approach. On the other hand, a fixed resolution value of $\rho = 4$ would lead to 15 grid points. To formalize this approach, we define threshold probability values, $[\psi_1, \dots, \psi_n]$, over the first component of the belief states, π_0 , and assign specific resolution values $[\rho_1, \dots, \rho_n]$ for the intervals defined by these thresholds. For instance, for the grid construction method used to generate the above $\mathcal{G}^{\text{variable}}$, the threshold value vector is $[0.5, 0]$, and the resolution value vector is $[4, 2]$.

3.3.2 LP model for multi-objective CPOMDP

The grid-based approximation that we describe above reduces a POMDP to an approximate MDP (Sandikçi, 2010). That is, the approximate model that is characterized by the value functions in (4) corresponds to an MDP model where $\mathbf{b} \in \mathcal{G}$ are the states. The transition probabilities between the states (i.e., grid points) can be obtained from the POMDP belief states, observation probabilities, transition probabilities, and β -values as follows:

$$f_{k\ell}^{ta} = \begin{cases} \sum_{\theta \in \mathcal{O}} \sum_{i \in \mathcal{S}} \sum_{j \in \mathcal{S}} \beta_{k\ell}^{ta\theta} b_i^k z_{i\theta}^{ta} p_{ij}^{ta} & \text{if } a = \mathbb{W}, \theta \in \mathcal{O}, \text{ or } a \neq \mathbb{W}, \theta = \theta^-, \\ \sum_{\theta \in \mathcal{O}} \sum_{j \in \mathcal{S}} \beta_{k\ell}^{ta\theta} b_0^k z_{0\theta}^{ta} p_{0j}^{ta} & \text{if } a \neq \mathbb{W} \text{ and } \theta = \theta^+, \end{cases}$$

where $\beta_{k\ell}^{ta\theta}$ corresponds to the convex combination weight for the grid point \mathbf{b}^ℓ for the updated belief state $(\mathbf{b}^k)'$ when the update is performed based on action a and observation θ at time t . Note that f values can be precalculated and stored for later usage.

By using a similar approximation mechanism, we can reduce the CPOMDP defined by (3) to an approximate constrained MDP. Let x_{tka} represent the *occupancy measures*, which specify the fraction of time that the patient occupies the belief state $\mathbf{b}^k \in \mathcal{G}$ at time $t \in \mathcal{T}$ and takes action $a \in \mathcal{A}$. We can formulate the following LP model for the approximate MDP:

$$\max \{h_1, -h_2\} \quad (5a)$$

$$\text{s.t. } \sum_{a \in \mathcal{A}} x_{0ka} = \delta_k, \quad k \in \mathcal{K}, \quad (5b)$$

$$\sum_{a \in \mathcal{A}} x_{tka} - \sum_{a \in \mathcal{A}} \sum_{\ell \in \mathcal{K}} f_{\ell k}^{t-1a} x_{t-1\ell a} = 0, \quad k \in \mathcal{K}, \quad 0 < t < T, \quad (5c)$$

$$x_{Tk} - \sum_{a \in \mathcal{A}} \sum_{\ell \in \mathcal{K}} f_{\ell k}^{T-1a} x_{T-1\ell a} = 0, \quad k \in \mathcal{K}, \quad (5d)$$

$$\sum_{t < T} \sum_{k \in \mathcal{K}} \sum_{a \in \mathcal{A}} \sum_{i \in \mathcal{S}} b_i^k c_i^{ta} x_{tka} \leq C, \quad (5e)$$

$$x_{Tk} \geq 0, \quad x_{tka} \geq 0, \quad a \in \mathcal{A}, \quad k \in \mathcal{K}, \quad t < T. \quad (5f)$$

We have two optimization objectives in this model, h_1 and h_2 , which correspond to expected total QALY and expected lifetime risk, respectively. The constraints specified by (5b) link the occupancy measures to the initial belief distribution δ_k , $k \in \mathcal{K}$ over the grid points. The initial belief distribution can be selected in a way that $\sum_{k \in \mathcal{K}} \delta_k b^k = \pi^0$. The constraints in (5c) and (5d) establish the connection between the occupancy measures at successive decision epochs. Constraint (5e) imposes a budget limit of C over the decision horizon. That is, the expected total cost of the taken actions cannot exceed C .

QALY and lifetime risk objectives can be formulated as follows:

$$h_1 = \sum_{t < T} \sum_{a \in \mathcal{A}} \sum_{k \in \mathcal{K}} \sum_{i \in \mathcal{S}} b_i^k \omega_i^{ta} x_{tka} + \sum_{t < T} \sum_{a \neq \mathbb{W}} \sum_{k \in \mathcal{K}} \sum_{i \neq 0, i \in \mathcal{S}} b_i^k z_{i\theta}^{ta} \phi_i^t x_{tka} \\ + \sum_{k \in \mathcal{K}} \sum_{i \in \mathcal{S}} b_i^k \varphi_i x_{Tk}, \quad (6)$$

$$h_2 = \sum_{t < T} \sum_{k \in \mathcal{K}} \sum_{a \neq \mathbb{W}} \sum_{i \neq 0} b_i^k z_{i\theta}^{ta} q_{ti} x_{tka} + \sum_{t < T} \sum_{k \in \mathcal{K}} \sum_{a \neq \mathbb{W}} b_2^k z_{2\theta}^{ta} p_{23}^{ta} x_{tka} \\ + \sum_{t < T} \sum_{k \in \mathcal{K}} \sum_{\theta \in \mathcal{O}} b_2^k z_{2\theta}^{t\mathbb{W}} p_{23}^{t\mathbb{W}} x_{tk\mathbb{W}}. \quad (7)$$

The first component in (6) corresponds to the expected total QALYs except for the case the patient is diagnosed with cancer, whereas the second component calculates the post-diagnosis QALYs. The final component accounts for terminal rewards. In (7), the first component calculates the lifetime risk post-diagnosis where q_{ti} represents the probability of a patient dying due to cancer if she is diagnosed at time t in state i . The second component is for the case when the patient receives a screening test but the outcome is a false negative. The final component corresponds to the lifetime risk value when the patient takes the wait action. The straightforward approach is to linearize these two objectives by using appropriately selected weight values, (w_1, w_2) , to obtain $w_1 h_1 - w_2 h_2$ as the optimization objective. However, we also experiment with multi-objective optimization techniques to obtain the Pareto frontier.

The model presented in (5) does not guarantee that the resulting screening policy will be deterministic (Puterman, 2014). Instead, the optimal policies may be *randomized*: there may be more than one optimal action for a given grid point-time tuple. In circumstances where randomized policies are unacceptable, which is often the case in medical diagnosis, we can enforce deterministic policy constraints. We define binary variables ν_{tka} and incorporate the following constraints into (5) to ensure deterministic policies:

$$x_{tka} \leq \nu_{tka}, \quad t < T, \quad k \in \mathcal{K}, \quad a \in \mathcal{A}, \quad (8a)$$

$$\sum_{a \in \mathcal{A}} \nu_{tka} = 1, \quad t < T, \quad k \in \mathcal{K}, \quad (8b)$$

$$\nu_{tka} \in \{0, 1\}, \quad t < T, \quad k \in \mathcal{K}, \quad a \in \mathcal{A}. \quad (8c)$$

These constraints ensure that for each grid point-time tuple, exactly one action is recommended. Cevik et al. (2018) also propose constraints to obtain threshold-type policies, which can be useful for clinical practice. The threshold-type policies rely on the stochastic ordering of the belief states, and ensure that policies follow the threshold levels over the belief states (e.g., take wait action if the patient is at least 99% healthy – $\pi = [0.99, 0.004, 0.006]$). However, these constraints come with an extra computational burden, and we, therefore, do not consider them in our analysis.

The approximate model defined in (5) can be simplified significantly by only considering the *useful* grid points and eliminating those from the formulation that

are guaranteed to result in $x_{tka} = 0$, $\forall k \in \mathcal{G}$, $\forall a \in \mathcal{A}$ at a given time t . Specifically, some grid points are not visited in certain decision epochs, and they do not contribute to the optimization objectives. This makes it possible to set the corresponding x -variable value to 0. The following proposition formalizes this idea:

Proposition 1 *If at time $t \in \{1, \dots, T-1\}$ and grid index $k \in \mathcal{K}$ we have*

$$f_{\ell k}^{t-1a} x_{tka} = 0, \quad \forall a \in \mathcal{A}, \ell \in \mathcal{K}$$

then, for all $a \in \mathcal{A}$, $x_{tka} = 0$.

Proof

From (5c) we have

$$\sum_{a \in \mathcal{A}} x_{tka} = \sum_{a \in \mathcal{A}} \sum_{\ell \in \mathcal{K}} f_{\ell k}^{t-1a} x_{t-1\ell a}$$

by Proposition 1, this becomes

$$\sum_{a \in \mathcal{A}} x_{tka} = 0$$

from (5f), which states

$$x_{tka} \geq 0$$

the only solution is

$$x_{tka} = 0, \quad a \in \mathcal{A}$$

□

We take that the grid point k is not useful at time t if it satisfies the condition in Proposition 1. In the model defined by (5), for each unuseful grid point, we can omit the $|\mathcal{A}|$ many corresponding x_{tka} variables and their associated constraints given in (5c). In the deterministic model, we can additionally omit $|\mathcal{A}|$ many binary ν_{tka} variables, as well as the two corresponding deterministic policy constraints given by (8a) and (8b).

4 Numerical Study

In this section, we discuss the parameter estimation procedures and present the results from our numerical study. Through detailed experiments, we first assess the performance of the grid-based approximations for the unconstrained POMDP model of breast cancer screening problem. Then, we present results for the multi-objective POMDP model. Note that optimization models are implemented in Python using Gurobi 9.0 and experiments are performed on a Linux machine with an Intel i7-8700K processor and 64 GB of system RAM.

4.1 Parameter Estimation

An important input for our models is the disutility of various screening and diagnostic outcomes. In this respect, we consider the following disutility values: 0.5 days for mammography, 2 days for mammography+MRI, 1 day for mammography+ultrasound, 28 days for TP and FP screening results (Sandikci et al., 2018). Furthermore, we set the terminal rewards for a patient at age 100, φ_i , to 2.5, 1.2, and 0.5 for being healthy, having in-situ cancer, and having invasive cancer, respectively (Ayer et al., 2012). Transition probabilities for average-risk (AR) and high-risk (HR) patients are obtained from the studies of Maillart et al. (2008) and Cevik et al. (2018), and the observation probabilities (i.e., sensitivity and specificity values for each action) are obtained from the studies of Ayer et al. (2012) and Sandikci et al. (2018). We note that an HR patient is 2–4 times more likely to get cancer than an AR patient. In terms of test performance, mammography+MRI has the highest sensitivity and the lowest specificity, whereas mammography+ultrasound has the highest specificity among these three tests. Post-cancer life expectancy values are also estimated similar to the estimations in Ayer et al. (2012), which are based on the methods by Arias (2014) and Siegel et al. (2014). Costs for mammography, mammography+MRI, and mammography+ultrasound actions are taken as \$80, \$200, and \$150, respectively. The starting belief states for the patients are estimated by using the breast cancer risk assessment tool provided on NCI's website¹.

4.2 Performance Evaluation

The performance of the grid-based approximation can be significantly impacted by the grid set composition. Typically, as the grid size increases, policies generated by the approximation methods get closer to the ones generated by the exact solution methods (e.g., Monahan's exhaustive enumeration algorithm). Accordingly, we first examine the performance of the grid-based approximations by using Lovejoy (1991)'s lower bound (LB) and upper bound (UB) mechanisms over the unconstrained POMDP model for our breast cancer screening problem. Note that the latter constitutes the baseline for our CPOMDP model provided in (5). We adopt the implementations provided by Kavaklıoglu and Cevik (2022) for the LB and UB methods.

Table 3 summarizes the performance for different grid sets based on an AR patient and by using the single objective model obtained by setting $w_1 = 1$ and $w_2 = 0$ (i.e., QALY maximization objective). We provide two sets of results, one for a single belief state, $\pi = [0.99, 0.004, 0.006]$, and the other is optimality gap statistics over 100 belief states randomly sampled according to the same resolution threshold vector ($\psi = [0.96, 0.80, 0]$) used for constructing all the grid sets. The optimality gap value for a specific belief state is calculated as $\text{Gap} (\%) = (\text{UB} - \text{LB})/|\text{LB}|$.

These results show that the gap values drop considerably as we increase the number of grid points in the variable resolution uniform grid construction method. In terms of CPU run times, the UB method is significantly worse than the LB

¹ <http://www.cancer.gov/bcrisktool/>

method and Monahan's algorithm (ME). Note that both the LB method and ME rely on the piece-wise linear value function representation for POMDPs (i.e., $Q^*(\boldsymbol{\pi}) = \max_m \{\boldsymbol{\pi} \cdot \boldsymbol{\alpha}^m\}$), and effectively employ $\boldsymbol{\alpha}$ -vectors to represent the model solutions. Accordingly, the LB method achieves similar values to those generated using ME even for small grid sets. On the other hand, the UB method repeatedly calculates β -values to achieve a reduction of the POMDP to a corresponding MDP, which leads to a significant increase in computational overhead. While the gap significantly tightens as we approach \mathcal{G}_3 , there is a negligible difference between the results obtained for \mathcal{G}_3 and \mathcal{G}_4 . As such, we set \mathcal{G}_3 , which uses $\boldsymbol{\rho} = [500, 50, 5]$ and $\boldsymbol{\psi} = [0.96, 0.8, 0]$, as our *default* grid set in the subsequent experiments.

Table 3: Effect of different resolution values for the variable resolution uniform grid construction method.

Grid Specification	Grid ID and $\boldsymbol{\rho}$	LB		ME		UB		Gap (%)		
		$ \mathcal{G} $	QALY	CPU	QALY	CPU	QALY	CPU	Min	Mean
\mathcal{G}_1 : (100, 25, 5)	51	40.210	8.5	40.213	943.9	40.293	114.7	0.0	0.077	0.201
\mathcal{G}_2 : (250, 50, 5)	144	40.212	50.2	-	-	40.231	679.7	0.0	0.017	0.052
\mathcal{G}_3 : (500, 50, 5)	309	40.213	285.5	-	-	40.216	3820.1	0.0	0.003	0.007
\mathcal{G}_4 : (1000, 50, 5)	939	40.213	8808.1	-	-	40.214	33775.1	0.0	0.001	0.002

*: QALY values are for the target belief state $\boldsymbol{\pi} = [0.99, 0.004, 0.006]$

†: resolution threshold vector is $\boldsymbol{\psi} = [0.96, 0.8, 0]$

‡: gap values are calculated over 100 randomly sampled evaluation grid points

We provide detailed results for the default grid set using five different belief states in Table 4. As expected, the QALY values decrease as the health status of a patient deteriorates (as indicated by the belief states with smaller π_0 values). We also find that both the LB and UB methods generate results that are very close to that of ME.

Table 4: QALY values for selected belief points for AR patients ($\boldsymbol{\rho} = [500, 50, 5]$).

Belief Point	LB	ME	UB
1.000, 0.000, 0.000	40.327	40.328	40.330
0.990, 0.004, 0.006	40.213	40.213	40.216
0.985, 0.006, 0.009	40.162	40.162	40.164
0.975, 0.012, 0.013	40.086	40.087	40.089
0.950, 0.018, 0.032	39.787	39.787	39.789

We next employ the default grid set for solving the unconstrained POMDP model by using the corresponding integer programming formulation, i.e., model (5) with the single objective h_1 , including the deterministic policy constraints, but excluding the budget constraint. Because our multi-objective CPOMDP models are constructed based on a similar formulation, this analysis sheds light on the corresponding run times. In this experiment, we also explore the impact of Proposition 1 for various grid set sizes. Figure 1a provides the percentage of useful grids at each

decision epoch, and Figure 1b compares the CPU run times on a logarithmic scale between the two configurations: using all of the grid points and using only the useful grid points. We note that, at the first decision epoch, all the grid points are used, as specified by the choice of δ . However, in the subsequent decision epochs, only a fraction of grid points are used/visited. We also find that the percentage of useful grid points decreases with $|\mathcal{G}|$. Across all the grid set sizes, we observe a significant performance boost in terms of run times, which tends to increase as $|\mathcal{G}|$ increases.

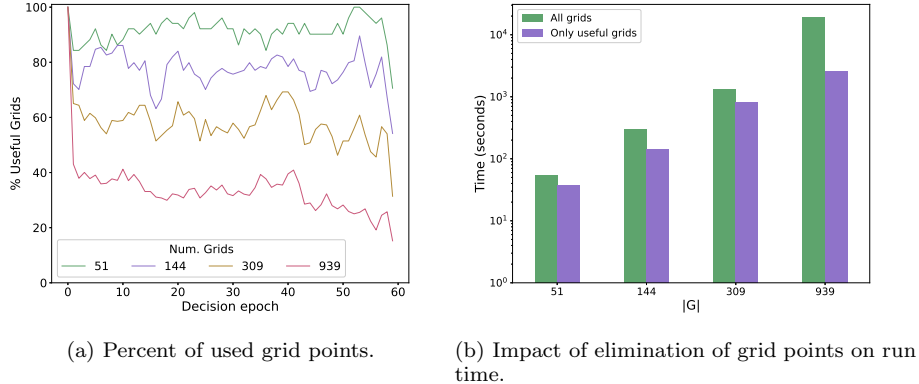


Fig. 1: Performance analysis results for unconstrained POMDP model solved using the corresponding integer programming formulation.

4.3 Multi-objective CPOMDP Results

We first solve the multi-objective CPOMDP model for three weight vectors: $w = [0.0, 1.0]$ (i.e., lifetime risk minimization), $w = [1.0, 0.0]$ (i.e., QALY maximization) and $w = [0.933, 0.067]$ (i.e., weighted objective optimization). Note that the weights in the weighted objective are determined via preliminary analysis. In this experiment, we do not impose any budget limits. Table 5 shows the baseline results for the breast cancer screening problem considering AR and HR patients. In Table 5a, we consider five different belief states to report the QALY and lifetime risk values.

We find that, as the belief state worsens (i.e., as the probability of being cancer-free decreases), QALY values decrease and the risk values increase, which is intuitive. We also observe that there is a noticeable trade-off between the QALY maximization and lifetime risk minimization objectives. Specifically, across the different belief states for AR patients, we observe that aggressive screening strategies lead to a decrease in lifetime risk by approximately 0.47%, but these strategies also result in a drop of 0.21 QALYs (i.e., 2.5 months). This can be explained by

the various disutilities (e.g., FP test results) associated with screening. We observe similar trends for HR patients as well. As expected, HR patients experience lower QALYs and a higher lifetime risk due to the elevated likelihood of developing breast cancer. On average, HR patients have a slightly lower QALY loss for a similar amount of lifetime risk reduction (0.17 QALY decrease for a 0.46% reduction in lifetime risk). This is mainly because the disutilities associated with screening are suppressed by the increased benefit of screening in terms of breast cancer mortality reduction, which lead to higher QALY values.

Table 5: Multi-objective POMDP results obtained for fixed objective weights (analysis exclude budget limits).

(a) AR patient						
Belief	$w = [0.000, 1.000]$		$w = [0.933, 0.067]$		$w = [1.000, 0.000]$	
	QALY	Risk (%)	QALY	Risk (%)	QALY	Risk (%)
1.000, 0.000, 0.000	40.113	3.776	40.293	3.861	40.330	4.256
0.990, 0.004, 0.006	40.003	4.151	40.179	4.240	40.216	4.632
0.985, 0.006, 0.009	39.955	4.338	40.127	4.421	40.164	4.821
0.975, 0.012, 0.013	39.883	4.650	40.053	4.731	40.089	5.118
0.950, 0.018, 0.032	39.591	5.711	39.754	5.791	39.789	6.168

(b) HR patient						
Belief	$w = [0.000, 1.000]$		$w = [0.933, 0.067]$		$w = [1.000, 0.000]$	
	QALY	Risk (%)	QALY	Risk (%)	QALY	Risk (%)
0.989, 0.003, 0.008	39.601	7.446	39.760	7.545	39.784	7.929
0.977, 0.008, 0.015	39.492	7.850	39.646	7.941	39.670	8.320
0.950, 0.018, 0.032	39.231	8.798	39.379	8.889	39.402	9.256
0.930, 0.028, 0.042	39.071	9.419	39.215	9.509	39.238	9.868
0.920, 0.033, 0.047	38.991	9.729	39.133	9.818	39.155	10.174

We next experiment with the multi-objective CPOMDP models by considering varying budget levels for AR and HR patients. We adopt two different approaches to solve the resulting approximate model: selecting a large number (100) of distinct weight values to solve the model using the weighted objective, and applying the ϵ -constraint method. Figures 2 and 3 show the results for AR and HR patients, respectively. As expected, repeatedly solving the model using the weighted objective — a naive approach to multi-objective optimization — fails to identify the majority of the values on the Pareto frontier. On the other hand, the ϵ -constraint method performs well in this regard, and helps to quantify the trade-offs between the QALY maximization and lifetime risk minimization objectives.

When the budget level is low, the trade-off between QALY and lifetime risk is less pronounced for AR patients. For $C = 200$, QALY values range between 40.09 and 40.13 (i.e., ± 0.04 years) and risk values range between 4.96% and 5.22% (i.e., $\pm 0.26\%$). On the other hand, for $C = 1,000$, QALY values range between 40.16 and 40.21 (i.e., ± 0.05 years) and risk values range between 4.44% and 4.80% (i.e.,

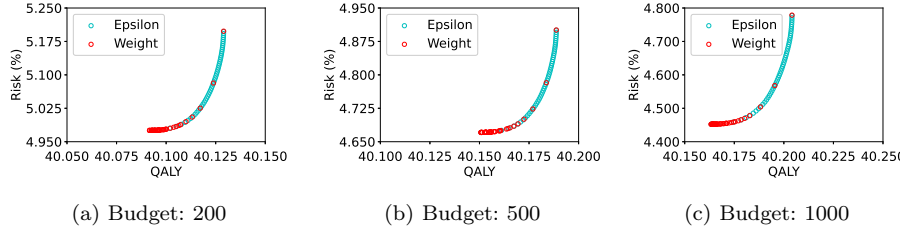


Fig. 2: Results with weighted objective and ϵ -constraint methods for various budget levels for AR patients (patient starting belief state is $[0.99, 0.004, 0.006]$).

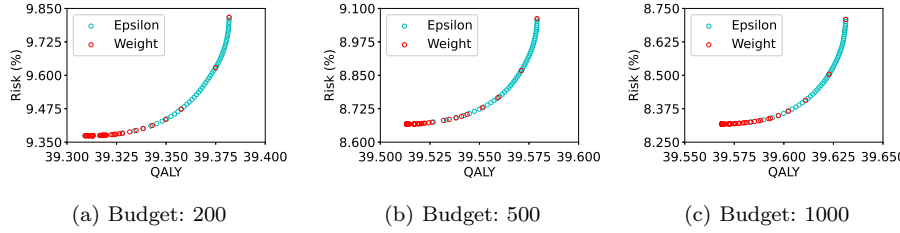


Fig. 3: Results with weighted objective and ϵ -constraint methods for various budget levels for HR patients (patient starting belief state is $[0.977, 0.008, 0.015]$).

$\pm 0.36\%$). This is mainly because, when the budget is higher, patients can opt to have more frequent screenings or to supplement their mammography with an MRI, which reduces the lifetime risk (due to its higher sensitivity) at the expense of reduced QALYs (due to its lower specificity that leads to increased FPs). The QALY versus lifetime risk trade-off is more pronounced across different budget levels for the HR patients as shown in Figure 3. This can again be attributed to their elevated likelihood of developing breast cancer. QALY values are negatively impacted by the increased probability of breast cancer death, which has a higher correlation to lifetime risk in the case of HR patients. That is, since the HR patients are more likely to develop cancer, they are also more likely to die of cancer. Accordingly, a wider range of QALY and lifetime risk outcomes are possible for HR patients, e.g., by carefully timing the available screenings and the screening modalities. For instance, screening at earlier ages can help increase the QALYs by extending the expected remaining lifetime at those ages, while screening between the ages of 50 and 70 (i.e., the ages when most cancer cases occur) can be more impactful in terms of reducing lifetime risk of breast cancer.

Figures 4 and 5 compare the performance of multi-objective CPOMDP policies obtained for three distinct objective weight configurations against the following fixed-interval (i.e., rule-based) policies: annual mammography screenings (A), biannual mammography screenings (B), biannual mammography screenings supplemented with MRI (B+R), and biannual mammography screenings supplemented with ultrasound (B+U). Note that these results are collected by using a discrete-event simulation model that involves simulating the lifetime of 100,000

patients. Figure 4a shows the relative QALY gain for each policy compared to no screening for AR patients. We observe that a budget of just 200 can be used to increase the QALYs above several rule-based screening strategies, with a budget of just 500 outperforming every rule-based policy in terms of QALYs. This demonstrates that using fewer screenings as prescribed by the CPOMDP model is sufficient in maximizing the QALY values for the AR patients. However, we observe in Figure 4b that the frequent screenings associated with rule-based policies tend to outperform budgeted policies when attempting to minimize risk. This is an expected result, as there is no detriment to overscreening when attempting to minimize risk. Figure 4c shows a significant difference in budgets used between the budgeted policies and the rule-based ones, with annual mammographies using nearly 2.5 times the maximum budget (i.e., \$1,000) with only a 0.25% improvement in lifetime risk. We observe that CPOMDP policies may exceed their budget. Here, each of the policies generated using a budget of \$1,000 exceed this budget in simulations by about 10%. Note that exceeding the imposed budget limits in a simulation environment can be attributed to the employed grid-based approximation scheme, as the approximate LP/MIP model only optimizes over the pre-defined grid points. Similar observations regarding the drawbacks of grid-based approximations for CPOMDPs were also made by Poupart et al. (2015).

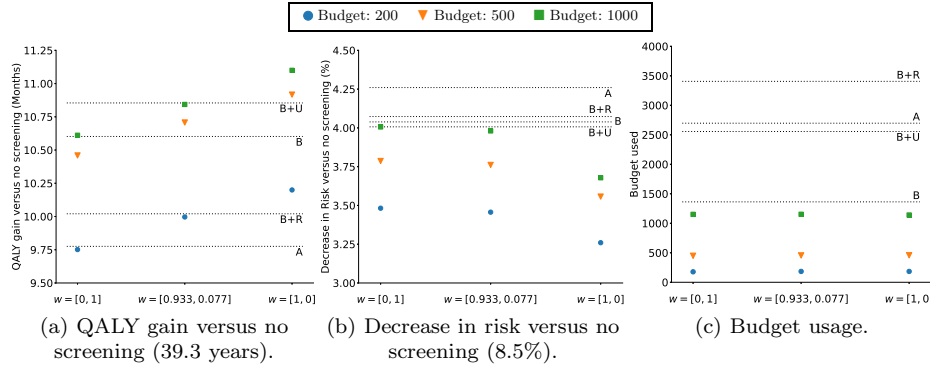


Fig. 4: Comparative analysis against fixed-interval policies for AR patients.

In contrast to the results for the AR patients, we observe in Figure 5a that the rule-based policies perform similar to one another with respect to maximizing QALYs in case of HR patients. We also observe that the maximum gain in QALYs is more than double that of AR patients. Unlike in the case of AR patients, a budget of 200 does not produce any competitive policies, as in both Figures 5a and 5b it is well separated from the other policies. However, a budget of 200 is still a significant improvement over no screening, and it is the most valuable policy per dollar spent. Interestingly, the gap between the best budgeted policy and the best rule-based policy with respect to risk minimization is about 0.25%, the same as in the AR patient case despite a nearly doubled reduction in risk. We observe in Figure 5c that rule-based policies for HR patients tend to cost slightly less than for AR patients. This result occurs because HR patients are more likely to develop cancer and are therefore more likely to leave the decision process due

to diagnosis or death. In contrast, the budgeted policies tend to fully utilize the available budget for both AR and HR patients.

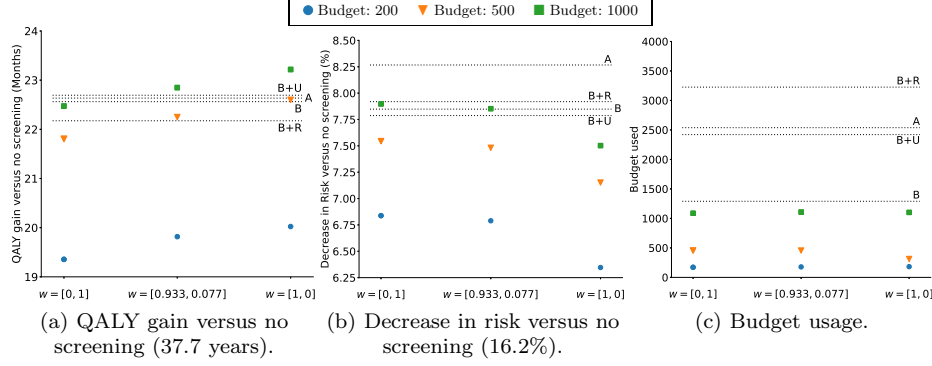


Fig. 5: Comparative analysis against fixed-interval policies for HR patients.

Table 6 summarizes the screening actions prescribed by various CPOMDP policies in a discrete-event simulation setting, as obtained by simulating the lifetime of 100,000 patients using our CPOMDP model data (e.g., starting belief states and transition/observation probabilities). As expected, with an infinite budget, the policies attempting to minimize lifetime risk employ aggressive screening using the highest sensitivity modality, i.e., mammography supplemented with MRI. In contrast, the QALY maximization objective tends to produce policies that screen less, and tend to use mammography supplemented with ultrasound when screening is necessary. Policies from weighted objective CPOMDP model lead to screening more aggressively than the QALY maximization policies, but also tend to use mammography supplemented with ultrasound when screening is necessary. We observe that budgeted policies all tend to use mammography alone, preserving their budget to allow for additional screenings. Remarkably, we observe that, while across each budget level for each patient type, the percentage of mammography actions taken is very similar, the results in Figures 4 and 5 clearly show that these policies are significantly different. These results show that the timing of screenings (the age that they were recommended/received) contributes significantly to both QALYs and lifetime risk.

Table 6: Percentage of screening actions taken for varying objectives, budgets, and patient types (the remaining percentage is the percentage of wait actions taken).

Patient	Budget	$w = [0.000, 1.000]$				$w = [0.933, 0.077]$				$w = [1.000, 0.000]$			
		Cost	% M	% M&U	% M&R	Cost	% M	% M&U	% M&R	Cost	% M	% M&U	% M&R
AR	200	177.6	6.54	0.00	0.00	184.0	6.77	0.00	0.00	184.0	6.77	0.00	0.00
	500	448.8	16.55	0.00	0.00	455.2	16.79	0.00	0.00	457.6	16.88	0.00	0.00
	1000	1151.2	42.56	0.00	0.00	1152.8	42.63	0.00	0.00	1140.3	21.02	11.26	0.00
	Inf.	5987.6	5.40	0.00	86.63	3744.9	0.68	73.33	0.21	2529.9	0.53	49.63	0.00
HR	200	171.2	6.64	0.00	0.00	177.6	6.89	0.00	0.00	181.6	7.05	0.00	0.00
	500	455.2	17.74	0.00	0.00	455.2	17.73	0.00	0.00	312.0	12.13	0.00	0.00
	1000	1087.2	42.58	0.00	0.00	1108.0	43.42	0.00	0.00	1101.6	43.18	0.00	0.00
	Inf.	5874.8	0.35	3.28	89.92	4650.5	0.16	93.35	3.18	3977.6	0.38	79.07	3.15

5 Conclusion and Future Work

In this study, we present a multi-objective constrained partially observable Markov decision process model for the breast cancer screening problem, which involves three partially observable health states and three screening modalities. We employ grid-based approximation methods to formulate an approximate mixed-integer linear programming model, which enables solving the multi-objective CPOMDP model using the ϵ -constraint method. We improve the solvability of this approximate model by eliminating unuseful grid points from the formulation, which leads to substantial gains in terms of CPU run times. We conduct detailed experiments to assess the trade-off between the QALY and lifetime risk optimization objectives. Being able to quantify such trade-offs can help health policy makers in designing more informed personalized screening policies.

Our research has certain limitations which can be, in part, addressed in future studies. First, because of the computational challenges, our baseline POMDP model is limited to only three health states. Patients' adherence behaviours as well as dynamic risk factors such as breast density can be incorporated into the state space to have a more representative model for the breast cancer screening problem. Secondly, imposing the budget limits for personalized screening involves setting the constraints over the lifetime of the patients. This approach might limit the adoption of these policies in practice, because it would be difficult to keep track of the patients over their lifetimes. On the other hand, our models also guide the policy makers in terms of which screening ages are more important when there are limited available resources. Such insights can be particularly useful in settings when the governments or institutions would need to carefully allocate screening resources to maximize early detection of cancer. Lastly, the budget constraints imposed in our formulations only account for screening and disregard various other costs including those of diagnostic tests and treatment. A more complex CPOMDP formulation can be developed in the future to account for these costs.

References

ACS (2019) Breast cancer early detection and diagnosis. <https://www.cancer.org/content/dam/CRC/PDF/Public/8579.00.pdf>

Akhavan-Tabatabaei R, Sánchez DM, Yeung TG (2017) A Markov decision process model for cervical cancer screening policies in colombia. *Medical Decision Making* 37(2):196–211

Alagoz O, Chhatwal J, Burnside ES (2013) Optimal policies for reducing unnecessary follow-up mammography exams in breast cancer diagnosis. *Decision Analysis* 10(3):200–224

Arias E (2014) United states life tables, 2010. *National Vital Statistics System* 63(7):1–63

Ayer T (2015) Inverse optimization for assessing emerging technologies in breast cancer screening. *Annals of Operations Research* 230(1):57–85

Ayer T, Alagoz O, Stout NK (2012) OR Forum—A POMDP approach to personalize mammography screening decisions. *Operations Research* 60(5):1019–1034, DOI 10.1287/opre.1110.1019, URL <https://doi.org/10.1287/opre.1110.1019>, <https://doi.org/10.1287/opre.1110.1019>

Ayer T, Alagoz O, Stout NK, Burnside ES (2016) Heterogeneity in women's adherence and its role in optimal breast cancer screening policies. *Management Science* 62(5):1339–1362

Ayvacı MUS, Alagoz O, Burnside ES (2012) The effect of budgetary restrictions on breast cancer diagnostic decisions. *Manufacturing & Service Operations Management* 14(4):600–617, DOI 10.1287/msom.1110.0371, URL <https://pubsonline.informs.org/doi/abs/10.1287/msom.1110.0371>, <https://pubsonline.informs.org/doi/pdf/10.1287/msom.1110.0371>

Ayvacı MUS, Alagoz O, Ahsen ME, Burnside ES (2018) Preference-sensitive management of post-mammography decisions in breast cancer diagnosis. *Production and Operations Management* 27(12):2313–2338

Bansal S, Deshpande V, Zhao X, Lauer JA, Meheus F, Ilbawi A, Gopalappa C (2020) Analysis of mammography screening schedules under varying resource constraints for planning breast cancer control programs in low-and middle-income countries: a mathematical study. *Medical Decision Making* 40(3):364–378

Barth Jr RJ, Gibson GR, Carney PA, Mott LA, Becher RD, Poplack SP (2005) Detection of breast cancer on screening mammography allows patients to be treated with less-toxic therapy. *American Journal of Roentgenology* 184(1):324–329

Çağlayan Ç, Ayer T, Ekwueme DU (2018) Assessing multi-modality breast cancer screening strategies for brca 1/2 gene mutation carriers and other high-risk populations. Available at SSRN 3139779 DOI <http://dx.doi.org/10.2139/ssrn.3139779>, URL <https://ssrn.com/abstract=3139779>

Cevik M, Ayer T, Alagoz O, Sprague BL (2018) Analysis of mammography screening policies under resource constraints. *Production and Operations Management* 27(5):949–972, DOI 10.1111/poms.12842, URL <https://onlinelibrary.wiley.com/doi/abs/10.1111/poms.12842>, <https://onlinelibrary.wiley.com/doi/pdf/10.1111/poms.12842>

Chen Q, Ayer T, Chhatwal J (2018) Optimal m-switch surveillance policies for liver cancer in a hepatitis c-infected population. *Operations Research* 66(3):673–696

Chhatwal J, Alagoz O, Burnside ES (2010) Optimal breast biopsy decision-making based on mammographic features and demographic factors. *Operations Research* 58(6):1577–1591

Coleman MP, Quaresma M, Berrino F, Lutz JM, De Angelis R, Capocaccia R, Baili P, Rachet B, Gatta G, Hakulinen T, et al. (2008) Cancer survival in five continents: a worldwide population-based study (CONCORD). *The Lancet Oncology* 9(8):730–756

DeSantis CE, Ma J, Gaudet MM, Newman LA, Miller KD, Goding Sauer A, Jemal A, Siegel RL (2019) Breast cancer statistics, 2019. *CA: A Cancer Journal for Clinicians* 69(6):438–451, DOI 10.3322/caac.21583, URL <https://acsjournals.onlinelibrary.wiley.com/doi/abs/10.3322/caac.21583>, <https://acsjournals.onlinelibrary.wiley.com/doi/pdf/10.3322/caac.21583>

Ebadí M, Akhavan-Tabatabaei R (2021) Personalized cotesting policies for cervical cancer screening: A pomdp approach. *Mathematics* 9(6):679

Elmore JG, Barton MB, Moceri VM, Polk S, Arena PJ, Fletcher SW (1998) Ten-year risk of false positive screening mammograms and clinical breast examinations. *New England Journal of Medicine* 338(16):1089–1096

Erenay FS, Alagoz O, Said A (2014) Optimizing colonoscopy screening for colorectal cancer prevention and surveillance. *Manufacturing & Service Operations Management*

Management 16(3):381–400

Fuller MS, Lee CI, Elmore JG (2015) Breast cancer screening: an evidence-based update. *The Medical Clinics of North America* 99(3):451

Gan K, Scheller-Wolf AA, Tayur SR (2019) Personalized treatment for opioid use disorder. Available at SSRN 3389539

Gopalappa C, Guo J, Meckoni P, Munkhbat B, Pretorius C, Lauer J, Ilbawi A, Bertram M (2018) A two-step markov processes approach for parameterization of cancer state-transition models for low-and middle-income countries. *Medical Decision Making* 38(4):520–530

Gray AM, Clarke PM, Wolstenholme JL, Wordsworth S (2011) Applied methods of cost-effectiveness analysis in healthcare, vol 3. Oxford University Press

Hajjar A, Alagoz O (2022) Personalized disease screening decisions considering a chronic condition. *Management Science* URL <https://doi.org/10.1287/mnsc.2022.4336>

Horiguchi M (2021) On an approach to evaluation of health care programme by markov decision model. In: *Modern Trends in Controlled Stochastic Processes*:, Springer, pp 341–354

Imani F, Qiu Z, Yang H (2020) Markov decision process modeling for multi-stage optimization of intervention and treatment strategies in breast cancer. In: *2020 42nd Annual International Conference of the IEEE Engineering in Medicine & Biology Society (EMBC)*, IEEE, pp 5394–5397

Kaiser CG, Dietzel M, Vag T, Froelich MF (2021a) Cost-effectiveness of mr-mammography vs. conventional mammography in screening patients at intermediate risk of breast cancer-a model-based economic evaluation. *European Journal of Radiology* 136:109355

Kaiser CG, Dietzel M, Vag T, Rübenthaler J, Froelich MF, Tollens F (2021b) Impact of specificity on cost-effectiveness of screening women at high risk of breast cancer with magnetic resonance imaging, mammography and ultrasound. *European Journal of Radiology* 137:109576

Kavaklıoglu C, Cevik M (2022) Scalable grid-based approximation algorithms for partially observable markov decision processes. *Concurrency and Computation: Practice and Experience* 34(5):e6743

Le QA (2016) Structural uncertainty of markov models for advanced breast cancer: a simulation study of lapatinib. *Medical Decision Making* 36(5):629–640

Lee E, Lavieri MS, Volk M (2019) Optimal screening for hepatocellular carcinoma: A restless bandit model. *Manufacturing & Service Operations Management* 21(1):198–212

Lee J, Kim GH, Poupart P, Kim KE (2018) Monte-Carlo tree search for constrained pomdps. In: *NeurIPS*, pp 7934–7943

Li W, Denton B, Morgan T (2021) Optimizing active surveillance for prostate cancer using partially observable markov decision processes. *Optimization Online*

Li Y, Zhu M, Klein R, Kong N (2014) Using a partially observable Markov chain model to assess colonoscopy screening strategies—a cohort study. *European Journal of Operational Research* 238(1):313–326

Lovejoy WS (1991) Computationally feasible bounds for partially observed markov decision processes. *Operations Research* 39(1):162–175

Madadi M, Zhang S, Henderson LM (2015) Evaluation of breast cancer mammography screening policies considering adherence behavior. *European Journal of Operational Research* 247(2):630

– 640, DOI <https://doi.org/10.1016/j.ejor.2015.05.068>, URL <http://www.sciencedirect.com/science/article/pii/S0377221715004804>

Maillart LM, Ivy JS, Ransom S, Diehl K (2008) Assessing dynamic breast cancer screening policies. *Operations Research* 56(6):1411–1427, DOI 10.1287/opre.1080.0614, URL <https://doi.org/10.1287/opre.1080.0614>, <https://doi.org/10.1287/opre.1080.0614>

Mandelblatt J, Stout N, Schechter C, van den Broek J, Miglioretti D, et al. (2016) Collaborative modeling of the benefits and harms associated with different U.S. breast cancer screening strategies. *Annals of Internal Medicine* 164(4):215–225

Molani S, Madadi M, Wilkes W (2019) A partially observable markov chain framework to estimate overdiagnosis risk in breast cancer screening: Incorporating uncertainty in patients adherence behaviors. *Omega* 89:40–53

Molani S, Madadi M, Williams DL (2020) Investigating the effectiveness of breast cancer supplemental screening considering radiologists' bias. *MedRxiv*

Narod SA, Iqbal J, Miller AB (2015) Why have breast cancer mortality rates declined? *Journal of Cancer Policy* 5:8 – 17, DOI <https://doi.org/10.1016/j.jcpo.2015.03.002>, URL <http://www.sciencedirect.com/science/article/pii/S2213538315000065>

O'Donoghue C, Eklund M, Ozanne EM, Esserman LJ (2014) Aggregate cost of mammography screening in the United States: comparison of current practice and advocated guidelines. *Annals of Internal Medicine* 160(3):145–153

Otten JWM, Witteveen A, Vliegen I, Siesling S, Timmer JB, IJzerman MJ (2017) Stratified breast cancer follow-up using a partially observable mdp. In: *Markov decision processes in practice*, Springer, pp 223–244

Otten M, Timmer J, Witteveen A (2020) Stratified breast cancer follow-up using a continuous state partially observable Markov decision process. *European Journal of Operational Research* 281(2):464–474

Petousis P (2019) Optimizing cancer screening with pomdps. PhD thesis, UCLA

Poupart P, Malhotra A, Pei P, Kim KE, Goh B, Bowling M (2015) Approximate linear programming for constrained partially observable markov decision processes. In: *Twenty-Ninth AAAI Conference on Artificial Intelligence*

Puterman ML (2014) *Markov decision processes: discrete stochastic dynamic programming*. John Wiley & Sons

Ralaidovy AH, Gopalappa C, Ilbawi A, Pretorius C, Lauer JA (2018) Cost-effective interventions for breast cancer, cervical cancer, and colorectal cancer: new results from who-choice. *Cost Effectiveness and Resource Allocation* 16(1):1–14

Sandıkçı B (2010) Reduction of a pomdp to an mdp. *Wiley Encyclopedia of Operations Research and Management Science*

Sandıkçı B, Cevik M, Schacht D (2018) Screening for breast cancer: The role of supplemental tests and breast density information. *Chicago Booth Research Paper* (18-03)

Saville CE, Smith HK, Bijak K (2019) Operational research techniques applied throughout cancer care services: a review. *Health Systems* 8(1):52–73

Siegel R, Ma J, Zou Z, Jemal A (2014) Cancer statistics, 2014. *CA: A Cancer Journal for Clinicians* 64(1):9–29

Siegel RL, Miller KD, Jemal A (2020) Cancer statistics, 2020. *CA: A Cancer Journal for Clinicians* 70(1):7–30, DOI 10.3322/caac.21590, URL <https://acsjournals.onlinelibrary.wiley.com/doi/abs/10.3322/caac.21590>, <https://acsjournals.onlinelibrary.wiley.com/doi/pdf/10.3322/caac.21590>

Sprague BL, Stout NK, Schechter C, Van Ravesteyn NT, Cevik M, Alagoz O, Lee CI, Van Den Broek JJ, Miglioretti DL, Mandelblatt JS, et al. (2015) Benefits, harms, and cost-effectiveness of supplemental ultrasonography screening for women with dense breasts. *Annals of Internal Medicine* 162(3):157–166

Tilanus-Linthorst M, Verhoog L, Obdeijn IM, Bartels K, Menke-Pluymers M, Egermont A, Klijn J, Meijers-Heijboer H, van der Kwast T, Brekelmans C (2002) A BRCA1/2 mutation, high breast density and prominent pushing margins of a tumor independently contribute to a frequent false-negative mammography. *International Journal of Cancer* 102(1):91–95

Tollens F, Baltzer PA, Dietzel M, Schnitzer ML, Kunz WG, Rink J, Rübenthaler J, Froelich MF, Kaiser CG (2021) Cost-effectiveness of mr-mammography in breast cancer screening of women with extremely dense breasts after two rounds of screening. *Frontiers in Oncology* p 3449

Tunc S, Alagoz O, Burnside E (2018) A new perspective on breast cancer diagnostic guidelines to reduce overdiagnosis. Available at SSRN 3270399

Vargas SA, Zhang S, Akhavan-Tabatabaei R (2015) Optimal decision making for breast cancer treatment in the presence of cancer regression and type ii error in mammography results. In: *Analysis, Modelling, Optimization, and Numerical Techniques*, Springer, pp 185–204

Waks AG, Winer EP (2019) Breast cancer treatment: A review. *Jama* 321(3):288–300

Witteveen A, Otten JW, Vliegen IM, Siesling S, Timmer JB, IJzerman MJ (2018) Risk-based breast cancer follow-up stratified by age. *Cancer Medicine* 7(10):5291–5298

Zhang J, Denton BT (2018) Partially observable markov decision processes for prostate cancer screening, surveillance, and treatment: a budgeted sampling approximation method. *Decision Analytics and Optimization in Disease Prevention and Treatment* pp 201–222

Zhang J, Denton BT, Balasubramanian H, Shah ND, Inman BA (2012a) Optimization of prostate biopsy referral decisions. *Manufacturing & Service Operations Management* 14(4):529–547

Zhang J, Denton BT, Balasubramanian H, Shah ND, Inman BA (2012b) Optimization of PSA screening policies: a comparison of the patient and societal perspectives. *Medical Decision Making* 32(2):337–349